

Raman spectra of bilayer graphene to probe the electrostatic environment

Paola Gava, Michele Lazzeri, A. Marco Saitta, and Francesco Mauri

IMPMC, Universit es Paris 6 et 7, CNRS, IPGP, 140 rue de Lourmel, 75015 Paris, France

(Dated: November 10, 2018)

The Raman shift, broadening, and relative Raman intensities of bilayer graphene are computed as functions of the electron concentration. We include dynamic effects for the phonon frequencies and we consider the gap induced in the band structure of bilayer graphene by an external electric field. We show that from the analysis of the Raman spectra of gated bilayer graphene it is possible to quantitatively identify the amount of charges coming from the atmosphere and from the substrate. These findings suggest that Raman spectroscopy of bilayer graphene can be used to characterize the electrostatic environment of few-layers graphene.

PACS numbers: 78.20.Bh,63.20.kd,78.30.Na,63.22.Np,81.05.Uw

I. INTRODUCTION

Graphene-based systems have recently attracted much attention from both the experimental and the theoretical point of view. Graphene is in fact characterized by a high carrier-mobility,^{1,2,3} which make those systems very exciting in view of future applications in nanoelectronics. In standard experimental setups, few-layers graphene (FLG) interacts with the environment through doping charges coming from the top (n_{top}) and from the bottom (n_{bot}) of the system. These charges determine the external electric field [$E = (n_{top} - n_{bot})|e|/(2\epsilon_0)$] and the total electron concentration ($n = n_{top} + n_{bot}$). E and n can thus be varied independently changing the charges from the two sides. n_{top} and n_{bot} can be intentionally induced by applying gate voltage differences between the system and the substrate, or via atoms/molecules deposition on top of the system. On the other hand, important unintentional doping charges are typically present. For instance, in FLG obtained by exfoliation on SiO_2 ^{1,2,3,4,5,6,7,8,9,10,11,12,13,14,15,16,17,18,19} or epitaxially grown on SiC ,²⁰ a charge transfer occurs between the substrate and the system, giving rise to a finite n_{bot} . In analogy, an additional n_{top} can be accidentally induced by the uncontrolled adsorption of molecules from the atmosphere.

Among FLG, the bilayer graphene is particularly interesting because it becomes a tunable band-gap semiconductor under the application of an electric field perpendicular to the system.^{4,5,6,20,21,22,23,24} In this context, the determination of the electric field is crucial in order to control the band-gap. Moreover, in graphene charge impurities originating from the top or from the substrate are the main source of scattering which reduces conduction performances.²⁵ Therefore, the determination of the charge transfer from the substrate or from the atmosphere is highly desirable for possible applications. Although experimental techniques allow to estimate the total electron concentration on the system, an accurate determination of the respective values of top and bottom charges has never been achieved so far, and can be particularly challenging, for instance, when doping is intention-

ally induced by deposition of molecules or polymeric electrolyte. In this work we use a tight binding (TB) model fitted on ab initio calculations to compute the Raman shift, broadening, and relative Raman intensity of the G modes in bilayer graphene, as a function of the electron concentration, for different values of top charges. In particular, the screening properties of the system in presence of an external electric field are described using ab initio density functional theory calculations (DFT), including the GW correction, while a TB model is used to reproduce the DFT calculated, GW corrected, band structure in the full Brillouin zone. We show that from the measured Raman spectra of bilayer graphene it is possible to determine the external charge distribution and thus the external electric field and the actual carriers concentration. This result is especially relevant since it shows that Raman spectroscopy, which is already widely used to investigate graphene-based systems, can be used to characterize the electrostatic environment of the sample. Moreover, since the charges coming from the atmosphere and the substrate are not expected to depend on the number of layers, Raman measurements on bilayer graphene can also be used to determine the origin and the amount of the unintentional doping of monolayer and few-layers graphene in the same environment.

The Raman spectra of monolayer graphene are characterized by a doubly-degenerate G peak (E_{2g} mode) at around 1580 cm^{-1} .^{7,8,9,10,11,12,13} This mode shows a strong electron-phonon coupling, which induces a phonon renormalization when n is varied. Therefore, Raman can be used to measure the total electron concentration. In bilayer graphene, in the absence of an external electric field the G peak splits, as in graphite, in a doubly-degenerate Raman active mode (E_{2g}) and a doubly-degenerate, Raman inactive, infra-red active mode (E_u). The E_{2g} mode is characterized by a symmetric in-phase displacement of the atoms in the two layers (Fig.1-a), whereas E_u is characterized by an antisymmetric out-of-phase displacement of those atoms (Fig.1-b). Most Raman measurements on bilayer graphene show a single G peak whose position is used, as in monolayer graphene, to measure the electron concentration on the system.^{11,14}

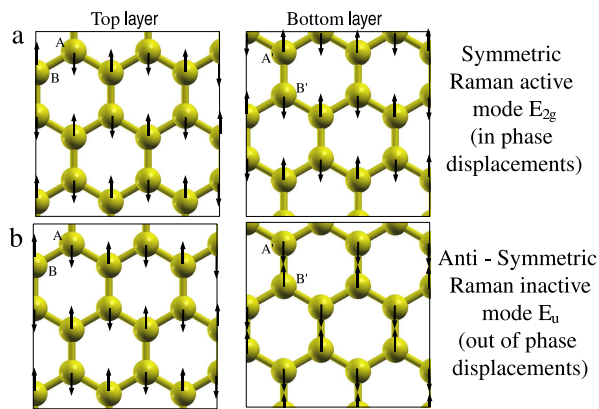


FIG. 1: (Color online) Schematic representation of the Raman active mode E_{2g} (a) and the Raman inactive mode E_u (b) in bilayer graphene. A,B are the inequivalent carbon atoms in the top layer, A' and B' are the inequivalent carbon atoms in the bottom layer. In a Bernal stacking configuration, A and A' are the superposed atoms.

Interestingly, the splitting of the G peak has been observed in the Raman spectra of bilayer graphene,¹⁵ and it has been recently attributed to symmetry breaking due to the application of an external electric field.³² Moreover, other experimental works recently reported on the infrared spectra of gated bilayer graphene.^{5,16,17,18,19} These findings suggest that a deep understanding of the behavior of a splitted G mode in gated bilayer graphene could lead to quantify not only the total electron concentration n but also the separate values of n_{top} and n_{bot} .

II. COMPUTATIONAL DETAILS

In order to calculate the electron-phonon coupling (EPC) component of the phonon frequencies, broadenings, and relative Raman intensities as functions of n and n_{top} , we consider the Γ phonon self-energy,^{26,27} projected onto the subspace of the two E_{2g} and the two E_u modes:

$$\Pi_{\mu\nu}(n_{top}, n) = \frac{\hbar}{M\omega_0 N_k} \sum_{\mathbf{k}, i, j} \frac{D_{ji}^\mu D_{ij}^\nu (f_{\mathbf{k}i} - f_{\mathbf{k}j})}{\epsilon_{\mathbf{k}i} - \epsilon_{\mathbf{k}j} + \hbar\omega_0 + i\eta}, \quad (1)$$

where the sum is on the electron wave vector \mathbf{k} and the electronic π bands i, j . $\mu, \nu=1,4$ are the phonon indexes, N_k is the number of \mathbf{k} vectors, and $f_{\mathbf{k}i}$ is the occupation of the electron state $|\mathbf{k}i\rangle$ with energy $\epsilon_{\mathbf{k}i}$. $D_{ij}^\mu = \langle \mathbf{k}i | \Delta H^\mu | \mathbf{k}j \rangle$ is the EPC and ΔH^μ is the Hamiltonian derivative with respect to the atomic displacement corresponding to the μ phonon. η equals 0.009 eV and M is the atomic mass.

From the phonon self-energy one can calculate only frequency variations due to changes in the electron concentration and in the band structure. In order to obtain

the absolute frequencies we use the following 4×4 matrix:

$$\Omega_{\mu\nu}(n_{top}, n) = \left(\omega_0 + \Delta\omega(n) - \Pi_0 + i\frac{\gamma_{an}}{2} \right) \delta_{\mu\nu} + \Pi_{\mu\nu}(n_{top}, n), \quad (2)$$

where $\omega_0=1581.5 \text{ cm}^{-1}$ is the experimentally measured frequency of the Raman active G peak in bilayer graphene, in absence of doping and electric field.¹⁴ γ_{an} is the contribution to the broadening of the G modes in graphene and graphite from the anharmonic phonon-phonon interaction, whose value is estimated to be 1.8 cm^{-1} .²⁸ Π_0 is the phonon self-energy of the doubly degenerate E_{2g} mode calculated for $n=0$ and $n_{top}=0$, and it is given by $\Pi_0 = \text{Re} [u_\mu^k \Pi_{\mu\nu}(0,0) u_\nu^k]$, where $k=1,2$ corresponds to the two E_{2g} modes and u_μ^k are the corresponding eigenvectors. In presence of doping charge the lattice parameter changes and the corresponding variation of the G modes frequencies can be obtained for zero electric field by ab initio calculations:²⁹ $\Delta\omega(n) = -5.75 \cdot 10^3 \Delta a(n) \text{ cm}^{-1}$, where $\Delta a(n)$ is the relative variation of the lattice parameter, as in Eq.(2) of Ref.²⁹ In this work we do not include in the phonon calculations the effects due to direct interaction of the system with adsorbates and with the substrate donating doping charge. However, as shown for intercalated graphite,^{36,37} we assume that this is not relevant also for the in-plane vibrational modes of bilayer graphene.

The eigenvalues of $\Omega_{\mu\nu}$ are of the form $(\omega_i + i\gamma_i/2)$, where ω_i is the frequency of phonon i and γ_i is the full width half maximum (FWHM), given by the EPC and the anharmonic phonon-phonon interaction. In the general case of finite n and n_{top} the four eigenmodes of $\Omega_{\mu\nu}$, ε_μ^i , are still two by two degenerate, but they are a superposition of the E_{2g} and E_u eigenmodes of the unbiased bilayer graphene. Their relative Raman intensities I_R^i are calculated as:

$$I_R^i = \frac{\sum_{k=1,2} |\varepsilon_\mu^i \cdot u_\mu^k|^2}{\sum_i \sum_{k=1,2} |\varepsilon_\mu^i \cdot u_\mu^k|^2}, \quad (3)$$

where $\sum_i I_R^i=1$.

We have shown that the screening properties of bilayer graphene under the application of an external electric field are characterized by inter- and intra-layer polarizations.²⁴ Most of the calculations of the band gap as a function of n and n_{top} are based on TB models,^{6,38} which usually consider only the inter-layer polarization, resulting in an overestimation of the band gap. In the present work the band structure of the π electrons [$\epsilon_{\mathbf{k}i}$ and $|\mathbf{k}i\rangle$ in Eq.(1)] is obtained using the scheme presented in Ref.²⁴ The band gap is computed by ab initio DFT calculations, including the GW corrections, and both inter- and intra-layer polarizations are fully taken into account. The full band structure of gated bilayer graphene is then computed using a TB model, which is able to reproduce all the important features of the DFT calculated, GW corrected bands, including the electron-hole asymmetry.

In order to compute ΔH^μ one needs to calculate the derivative of the tight binding Hamiltonian with respect

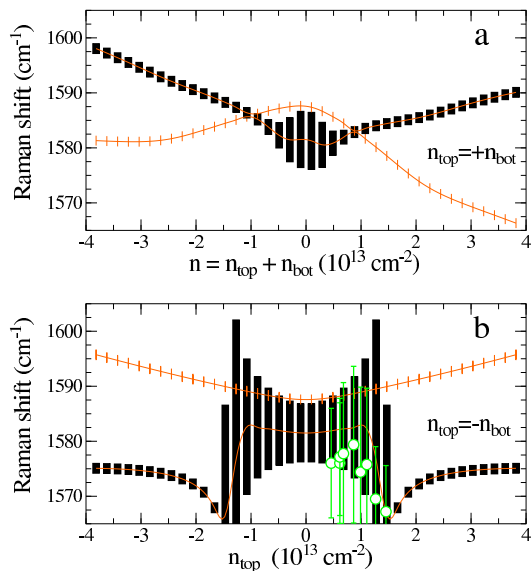


FIG. 2: (Color online) Raman shift in bilayer graphene for $n_{top} = n_{bot}$ and for $n_{top} = -n_{bot}$. Calculated values of the shifts are connected by lines. For a given value of n (panel a) or n_{top} (panel b) there are two phonon modes represented with two rectangles. The height of the rectangles is the FWHM and the areas are proportional to the relative Raman intensities (i.e. the integrated area of each peak) of the two modes. Thus, the ratio of the widths of the two rectangles is equal to the ratio of the maximum heights of the two Raman peaks. When the ratio is less than 0.1, the mode with the smallest intensity is colored in gray (red), otherwise is black. Circles are experimental results from Ref.¹⁷ and the errorbars represent the experimental FWHM.

to the atomic positions. However, only the variation of the first nearest-neighbors in-plane hopping parameters γ_1 turns out to be relevant, and this only term is thus included in ΔH^μ . The value we use for this quantity is 5.8 eV \AA^{-1} , which derives from the ab initio GW-calculated EPC at Γ for the E_{2g} mode in monolayer graphene.³⁰

III. RESULTS

In Fig.2-a we show the calculated Raman shift as a function of n , for the case $n_{top} = n_{bot}$, where the external electric field and the band-gap are kept fixed to zero, as theoretically studied in Ref.³¹ In this case the E_{2g} and E_u modes do not mix by symmetry. Analogously to monolayer graphene, the Raman active modes show a singularity when the Fermi energy is half of the phonon energy. In Fig.2-b we show the calculated Raman shifts for the case $n_{top} = -n_{bot}$, as a function of n_{top} . This is a special situation where the external electric field is varied while n is kept fixed to zero, as realized in recent infra-red experiments.^{5,17} In this case, the mixing between E_{2g} and E_u modes is weak due to the antisymmetric allocation of charges in the two layers. The Raman active modes show a singularity in the frequency and a divergence in the

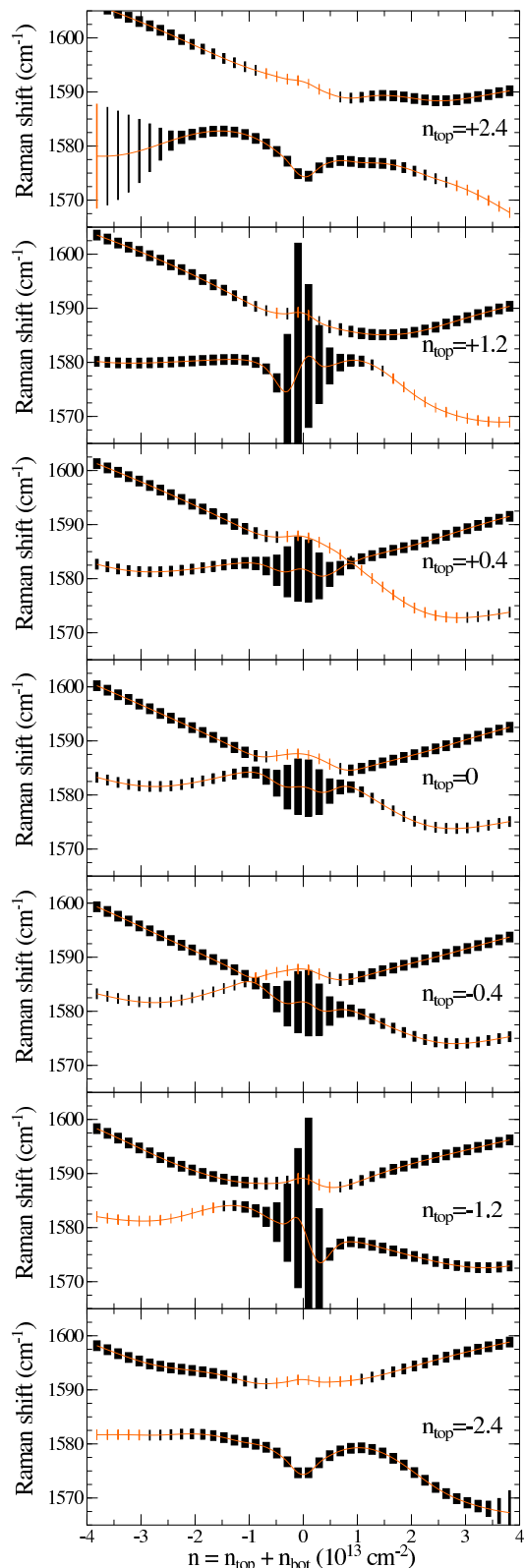


FIG. 3: (Color online) Raman shift in bilayer graphene as a function of the electron concentration n , for different values of n_{top} . See the caption of Fig.2.

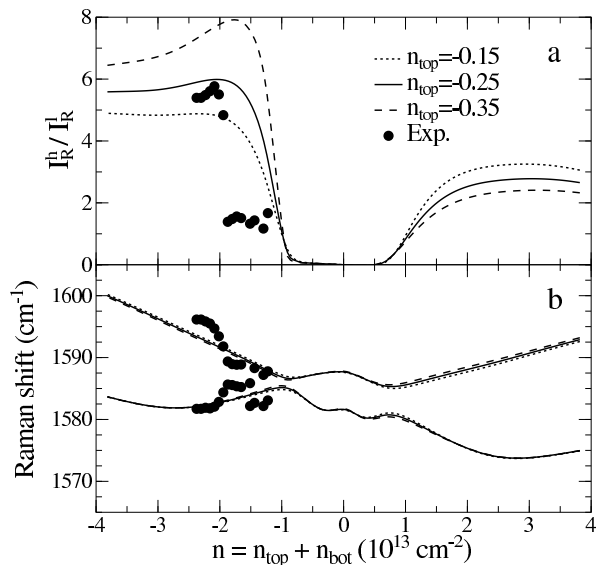


FIG. 4: Ratio between the relative Raman intensities of the highest and lowest mode, a, and Raman shift, b, as a function of n . Filled dots are experimental results from Ref.^{15,33}, shifted by $n^0 = -1.8 \cdot 10^{13} \text{cm}^{-2}$. Lines are the theoretical values for $n_{top} = -0.15, -0.25, -0.35 \cdot 10^{13} \text{cm}^{-2}$.

FWHM when the band-gap is of the order of the phonon energy.

In the most general situation the electric field and n are both finite. In Fig.3 we show the Raman shift of bilayer graphene as functions of n , for different values of n_{top} . In these cases, the E_{2g} and E_u modes do mix, and at certain values of n_{top} and n two modes become Raman visible. Our results show an asymmetry between positive and negative values of n_{top} . For instance, in the case $n_{top} = 2.4 \cdot 10^{13} \text{cm}^{-2}$ the FWHM of the lowest mode at $n \approx -4 \cdot 10^{13} \text{cm}^{-2}$ is higher than the same quantity for the case $n_{top} = -2.4 \cdot 10^{13} \text{cm}^{-2}$ at $n \approx 4 \cdot 10^{13} \text{cm}^{-2}$. This is due to the electron-hole asymmetry in the band structure, which is properly described in our calculations. Moreover, the asymmetry between positive and negative n is enhanced by the effect of the lattice spacing variation induced by the doping charge. Our results are qualitatively in agreement with recent calculations,³² based on TB model. They are however quantitatively different, because in our calculations we include the electron-hole asymmetry, the lattice spacing variation due to doping charge, and both inter- and intra-layer polarizations. The dependence on n of the frequencies, FWHM, and relative Raman intensities is strongly influenced by n_{top} , and on the basis of this observation we claim that the amount of uncontrolled n_{top} and n_{bot} can be estimated from the Raman spectra of bilayer graphene when two modes are observed.

We now compare our calculations to the experimental Raman spectra of bilayer graphene where the splitting of the G mode is reported.¹⁵ In this work charges are intentionally induced on the system by applying a gate voltage between the bilayer and the SiO_2 substrate. However,

unintentional n_{top} and n_{bot} arising from the atmosphere and the substrate can be present at zero gate voltage. By comparing the experimental and calculated Raman shifts as a function of n for different n_{top} , we estimate a total electron concentration at zero gate voltage $n^0 = -1.8 \cdot 10^{13} \text{cm}^{-2}$. In Fig.4-a and -b we show the ratio between the relative Raman intensities of the highest and lowest mode, and the Raman shifts, respectively, as a function of the electron concentration n , for different values of n_{top} . The former one strongly depends on n_{top} , while the frequency shifts have a weaker dependence. The best agreement between theory and experiments indicates an unintentional charge coming from the atmosphere $n_{top}^0 = -0.25 \cdot 10^{13} \text{cm}^{-2}$. From our estimate of n^0 , we deduce an unintentional charge from the substrate $n_{bot}^0 = n^0 - n_{top}^0 = -1.55 \cdot 10^{13} \text{cm}^{-2}$. The agreement between experimental data and theoretical results is good. However, we notice that the slope of the theoretical curves is underestimated with respect to the experimental ones. This could be possibly due to local desorption of molecules and doping variation induced by the laser light, or to hysteresis effects in the doping dependence on gate voltage.

Finally, in the right side of Fig.2-b, we compare our theoretical results to the experimental frequencies and broadenings from recent infra-red measurements in Ref.¹⁷, where the doping charge is kept fixed to zero and the electric field is varied. The agreement is excellent with our lower frequency mode. In our calculations, the lower mode has a weak projection on E_u . However, this mode is strongly coupled with the electrons, as testified by the large FWHM. Such coupling enhances the effective charges associated with E_u and increases the infra-red activity.^{18,34,35} Indeed, in Fig.3 of Ref.¹⁷ the measured infra-red intensity is maximum when the band-gap equals the phonon energy (about 0.2 eV), i.e. when the FWHM and thus the coupling of the mode with the electrons are maximum, while it decreases when the FWHM decreases.

IV. CONCLUSIONS

In summary, we have computed the Raman spectra of gated bilayer graphene, which is strongly influenced by the interaction with the environment. We claim that by the analysis of the splitting of the G mode in Raman measurements it is possible to estimate the amount of unintentional charges coming from the atmosphere and from the substrate. Here we compare our calculations with the only experimental data available on the G mode splitting in bilayer graphene, and we give an estimate of the unintentional charges coming from the environment in this experiment. In order to facilitate the comparison of new experimental results with our theoretical calculations, we provide as additional material a set of computed Raman shifts, FWHM, and relative Raman intensities as a function of n , for different values of n_{top} .³⁹

-
- ¹ K. S. Novoselov, A. K. Geim, S. V. Morozov, Jiang, Y. Zhang, S. V. Dubonov, I. V. Grigorieva, and A. Firsov, *Science* **306**, 666 (2004).
- ² K. S. Novoselov, A. K. Geim, S. V. Morozov, D. Jiang, M. Katsnelson, I. Grigorieva, S. Dubonov, and A. Firsov, *Nature* **438**, 197 (2005).
- ³ Y. Zhang, Y. Tan, H. L. Stormer, and P. Kim, *Nature* **438**, 201 (2005).
- ⁴ J. B. Oostinga, H. B. Heersche, X. Liu, A. F. Morpurgo, and L. M. K. Vandersypen, *Nature Mater.* **7**, 151 (2008).
- ⁵ Y. Zhang, T. Tang, C. Girit, Z. Hao, M. C. Martin, A. Zettl, M. F. Crommie, Y. R. Shen, and F. Wang, *Nature* **459**, 820 (2009).
- ⁶ E. V. Castro, K. S. Novoselov, S. V. Morozov, N. M. R. Peres, J. M. B. Lopes dos Santos, J. Nilsson, F. Guinea, A. K. Geim, and A. H. Castro Neto, *Phys. Rev. Lett.* **99**, 216802 (2007).
- ⁷ A. C. Ferrari, J. C. Meyer, V. Scardaci, C. Casiraghi, M. Lazzeri, F. Mauri, S. Piscanec, D. Jiang, K. S. Novoselov, S. Roth, et al., *Phys. Rev. Lett.* **97**, 187401 (2006).
- ⁸ S. Pisana, M. Lazzeri, C. Casiraghi, K. S. Novoselov, A. K. Geim, A. C. Ferrari, and F. Mauri, *Nature Mater.* **6**, 198 (2007).
- ⁹ C. Casiraghi, S. Pisana, K. S. Novoselov, A. K. Geim, and A. C. Ferrari, *Appl. Phys. Lett.* **91**, 233108 (2007).
- ¹⁰ C. Stampfer, F. Molitor, D. Graf, and K. Ensslin, *Appl. Phys. Lett.* **91**, 241907 (2007).
- ¹¹ A. Das, B. Chakraborty, S. Piscanec, S. Pisana, A. K. Sood, and A. C. Ferrari, *Phys. Rev. B* **79**, 155417 (2009).
- ¹² J. Yan, Y. Zhang, P. Kim, and A. Pinczuk, *Phys. Rev. Lett.* **98**, 166802 (2007).
- ¹³ A. Das, S. Pisana, B. Chakraborty, S. Piscanec, S. K. Saha, U. V. Waghmare, K. S. Novoselov, H. R. Krishnamurthy, A. K. Geim, A. C. Ferrari, et al., *Nature Nanotech.* **3**, 210 (2008).
- ¹⁴ J. Yan, E. A. Henriksen, P. Kim, and A. Pinczuk, *Phys. Rev. Lett.* **101**, 136804 (2008).
- ¹⁵ L. M. Malard, D. C. Elias, E. S. Alves, and M. A. Pimenta, *Phys. Rev. Lett.* **101**, 257401 (2008).
- ¹⁶ A. B. Kuzmenko, E. van Heumen, D. van der Marel, P. Lerch, P. Blake, K. S. Novoselov, and A. K. Geim, *Phys. Rev. B* **79**, 115441 (2009).
- ¹⁷ T.-T. Tang, Y. Zhang, C.-H. Park, B. Geng, C. Girit, Z. Hao, M. C. Martin, A. Zettl, M. F. Crommie, S. G. Louie, Y. R. Shen, and F. Wang, arXiv:0907.0419 (2009).
- ¹⁸ A. B. Kuzmenko, L. Benfatto, E. Cappelluti, I. Crassee, D. van der Marel, P. Blake, K. S. Novoselov, and A. K. Geim, arXiv:0906.2203 (2009).
- ¹⁹ L. M. Zhang, Z. Q. Li, D. N. Basov, M. M. Fogler, Z. Hao, and M. C. Martin, *Phys. Rev. B* **78**, 235408 (2008).
- ²⁰ T. Ohta, A. Bostwick, T. Seyller, K. Horn, and E. Rotenberg, *Science* **313**, 951 (2006).
- ²¹ E. McCann, *Phys. Rev. B* **74**, 161403(R) (2006).
- ²² H. Min, B. Sahu, S. K. Banerjee, and A. H. MacDonald, *Phys. Rev. B* **75**, 155115 (2007).
- ²³ M. Aoki and H. Amawashi, *Solid State Commun.* **142**, 123 (2007).
- ²⁴ P. Gava, M. Lazzeri, A. M. Saitta, and F. Mauri, *Phys. Rev. B* **79**, 165431 (2009).
- ²⁵ J.-H. Chen, C. Jang, S. Adam, M. S. Fuhrer, E. D. Williams, and M. Ishigami, *Nature Phys.* **4**, 377 (2008).
- ²⁶ P. B. Allen, *Phys. Rev. B* **6**, 2577 (1972).
- ²⁷ P. B. Allen and R. Silbergliitt, *Phys. Rev. B* **9**, 4733 (1974).
- ²⁸ N. Bonini, M. Lazzeri, N. Marzari, and F. Mauri, *Phys. Rev. Lett.* **99**, 176802 (2007).
- ²⁹ M. Lazzeri and F. Mauri, *Phys. Rev. Lett.* **97**, 266407 (2006).
- ³⁰ M. Lazzeri, C. Attaccalite, L. Wirtz, and F. Mauri, *Phys. Rev. B* **78**, 081406(R) (2008).
- ³¹ T. Ando, *J. Phys. Soc. Jpn.* **76**, 104711 (2007).
- ³² T. Ando and M. Koshino, *J. Phys. Soc. Jpn.* **78**, 034709 (2009).
- ³³ In Ref.¹⁵ the authors fit the raw experimental data with Lorentzians of variable FWHM. Here we re-fit data from Ref.¹⁵ for all gate voltages with two Lorentzians of fixed FWHM equal to 7 cm^{-1} , which is the value obtained in Ref.¹⁵ for large negative voltages, where the two peaks are well resolved. Our choice is justified by the fact that, according to our calculations, the EPC contribution to the FWHM is vanishing around $n^0 = -1.8 \cdot 10^{13} \text{ cm}^{-2}$, for all considered n_{top} (Fig.3). Thus, the increase in broadening observed in Ref.¹⁵ for positive value of gate voltage is not due to an increase of the decay rate (γ_i) but to the presence of two contributions of fixed width in the Raman peak, close in frequency but not exactly superimposed. The root mean square error obtained with the two fitting procedures are comparable.
- ³⁴ M. J. Rice, N. O. Lipari, and S. Strassler, *Phys. Rev. Lett.* **39**, 1359 (1977).
- ³⁵ M. J. Rice and H.-Y. Choi, *Phys. Rev. B* **45**, 10173 (1992).
- ³⁶ L. Boeri, G. B. Bachelet, M. Giantomassi, and O. K. Andersen, *Phys. Rev. B* **76**, 064510 (2007).
- ³⁷ M. Calandra and F. Mauri, *Phys. Rev. Lett.* **95**, 237002 (2005).
- ³⁸ E. McCann, *Phys. Rev. B* **74**, 161403(R) (2006).
- ³⁹ See EPAPS supplementary material at XXXX for computed Raman shifts, FWHM, and relative Raman intensities as a function of n and n_{top} .